Experiments on Turbulent Non-Newtonian Mass Transfer in a Circular Tube

O. C. Sandall, O. T. Hanna, K. Amarnath
Department of Chemical and Nuclear Engineering
University of California
Santa Barbara, CA 93106

Introduction

The problems of turbulent mass and heat transport in non-Newtonian duct flows are important in a number of industrial processes such as food processing, biochemical operations, and transport in polymer solutions. In the past there have been a number of studies of turbulent non-Newtonian heat transfer in ducts. But virtually no experimental data exist for turbulent non-Newtonian mass transfer in ducts. This is mentioned in a recent paper by Kawase and Ulbrecht (1982).

In an earlier study of turbulent Newtonian mass transfer, Kafes and Clump (1973) developed a useful experimental technique involving transport through a dialysis membrane. In the present work, a similar technique is used to study mass transfer in non-Newtonian fluids. The non-Newtonian fluids used were aqueous solutions of the polymer Carbopol-934. These solutions are nonelastic and their rheological properties are described well by the power law model. Overall mass transfer coefficients are measured for the transfer of CO_2 from a CO_2-saturated polymer solution circulated in the annulus, across a circular dialysis tube of 0.0157 m ID, to a polymer solution flowing through the dialysis tubing. Data are taken for each solution such that the mass transfer resistance due to the dialysis tube wall and the fluid in the annulus is constant, while the flow rate is varied inside the dialysis tube. Mass transfer coefficients for the tube side are obtained from the measured overall mass transfer coefficient by using a modified Wilson plot. The experimental results are correlated by means of an adaptation of the very general turbulent transport prediction equation of Sandall et al. (1980).

In a series of papers (Hanna and Sandall, 1972, 1978, 1982; Sandall et al., 1976, 1980, 1982, 1984; Sandall and Hanna, 1979; Hanna et a., 1981), two of the present authors have developed prediction formulas for turbulent mass or heat transfer based on an extended asymptotic expansion of the rigorous Lyon transport equation for the case of large Schmidt or Prandtl number. In the case of turbulent non-Newtonian heat transfer, this approach was used to develop the prediction formula of Sandall et al. (1976), which is:

$$\frac{\sqrt{f/2}}{St} = 12.5Pr^{2/3} + 1.24 \ln Pr + \frac{2.78}{n} \ln\left(\frac{Re\sqrt{f/2}}{90}\right) \quad (1)$$

In Sandall et al. (1980) it was shown that a single equation based on the asymptotic method provides an excellent prediction of Newtonian mass or heat transfer. This formula is:

$$\frac{\sqrt{f/2}}{St} = 12.5Pr^{2/3} - 7.85Pr^{1/3} + 3.61 \ln Pr + 5.8 + 2.78 \ln\left(\frac{Re\sqrt{f/2}}{90}\right) \quad (2)$$

Figure 1 shows a comparison of Eq. 2 with various sets of Newtonian heat and mass transfer data.

A comparison of the large Sc (or Pr) calculation procedure as applied to non-Newtonian vs. Newtonian transport is revealing. Equation 1 shows that the only explicit contribution of the non-Newtonian index n occurs in the last term on the right, which represents the turbulent "core" resistance to transport. It is natural to propose that the prediction of non-Newtonian transport be based on the use of Eq. 2 with non-Newtonian friction factor, Reynolds number, and Prandtl (Schmidt) number, along with employment of the core resistance of Eq. 1.

The result of this modification is Eq. 3:

$$\frac{\sqrt{f/2}}{St} = 12.5Pr^{2/3} - 7.85Pr^{1/3} + 3.61 \ln Pr + 5.8 + \frac{2.78}{n} \ln\left(\frac{Re\sqrt{f/2}}{90}\right) \quad (3)$$

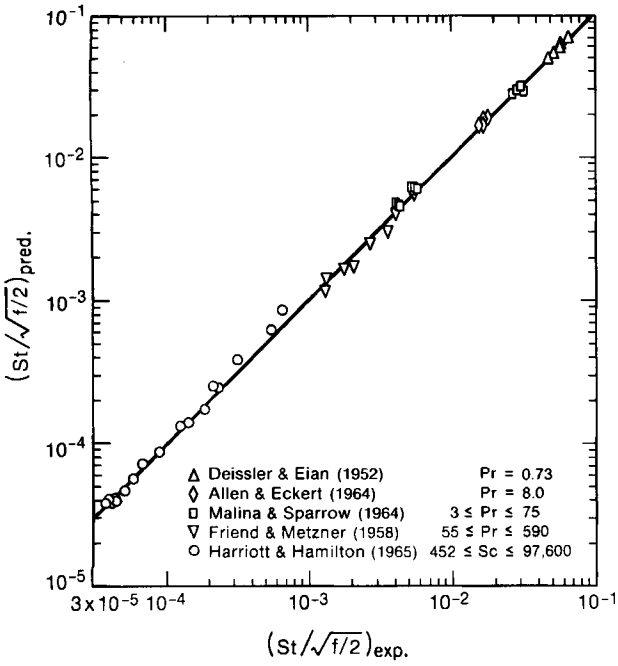

Figure 1. Comparison of Eq. 2 with various sets of Newtonian heat and mass transfer data.

Equation 3 reduces to Eq. 2 for Newtonian transport ($n = 1$). As shown later, Eq. 3 yields a very good correlation of our experimental data. For mass transfer Eq. 3 is used with the Schmidt number replacing the Prandtl number, and St is the Stanton number for mass transfer, k_i/v_b. The friction factor in Eq. 3 is that of Dodge and Metzner (1959), which is:

$$\frac{1}{\sqrt{f}} = \frac{4.0}{n^{0.75}} \log\left(Ref^{1-n/2}\right) - \frac{0.4}{n^{1.2}} \tag{4}$$

Experimental Apparatus and Procedure

The apparatus consisted of a column/tube contact section and ancillary circulation and measurement components as shown in Figure 2. The mass transfer column was constructed from a glass pipe, 1.83 m long and 0.0627 m ID. A cellulose dialysis tubing, 0.0158 m ID, was held in the center of this tube by two pieces of stainless steel tubing (0.0159 m dia.). The inlet stainless steel tube also served as a calming length to establish a fully developed velocity profile.

Flow in the dialysis membrane section was countercurrent to the annulus section flow; liquid from the stripping section reservoir entered the mass transfer column at the bottom after passing through a rotameter and entrance calming section. The enriched liquid leaving this column was discharged to the stripper. Liquid from the saturation section entered the column at the top after going through a rotameter and was discharged at the bottom and returned to the saturation section. A perforated baffle at the top of the column uniformly distributed the annulus section flow. A mercury manometer was connected between the dialysis membrane section and the annulus section at the top of the column in order to maintain a negligible pressure gradient between the two streams.

The stripping section consisted of a glass column, 0.102 m dia. and 0.915 m long, packed with 9.6×10^{-3} m glass Raschig rings to a height of 0.64 m. Stripping was carried out by means of compressed air flowing countercurrent to the direction of the liquid. The saturation section consisted of a glass cylindrical vessel of 0.305 m dia. and 0.47 m long. Bone-dry grade carbon dioxide gas was sparged through the liquid which, in turn, was agitated with a 0.075 m turbine impeller at a speed of 200 rpm to ensure proper mixing.

The temperature of the liquid in the entire system was kept steady at 25°C throughout the experiment by circulating water through cooling coils in the reservoirs of the stripping and saturation sections. Because of difficulty in controlling pressure difference, fragility of the membrane, and design of the apparatus,

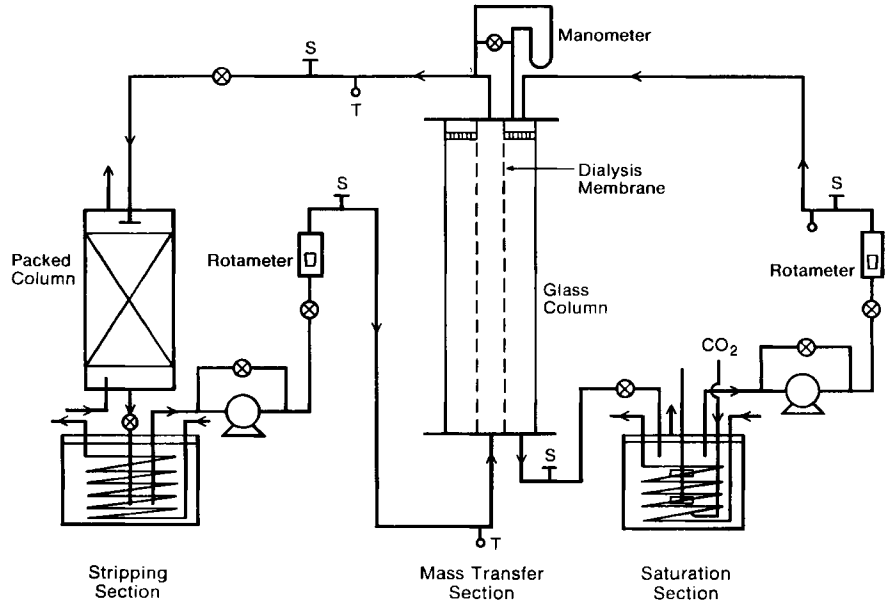

Figure 2. Schematic diagram of experimental apparatus.

Table 1. Rheological Properties of Aqueous Carbopol Solutions at 25°C

% Carbopol in Water	Flow Behavior Index, n	Consistency Index, K g/cm · s^{2-n}
0.25	0.902	0.0390
0.50	0.875	0.0610
0.55	0.854	0.1218

the maximum flow rate was about 2.5 gpm (0.16 L/s). Before installing the membrane, it was steeped in water for 24 h to increase its strength.

Liquid samples were pipeted out from the inlet and outlet sample ports of both the dialysis membrane and outside sections of the mass transfer column. A wet-chemistry technique was used for the analysis of carbon dioxide. Carbon dioxide was precipitated as barium carbonate from a solution of standardized barium chloride and sodium hydroxide. Excess sodium hydroxide was titrated to a phenolphthalein end point with hydrochloric acid on carbon-dioxide-free solutions. Care was taken to avoid loss of carbon dioxide to the atmosphere during the transfer of samples.

For measuring the diameter of the dialysis membrane, a sample tubing was first steeped in water for 24 h. The tube was filled with water and the outside diameter was measured at several places using a micrometer. The thickeness of this membrane was measured to obtain an internal diameter of 0.0158 ± 0.0001 m.

The rheological properties of the aqueous Carbopol solutions were determined using a capillary tube viscometer. The data are described well by the power law model. Table 1 summarizes the rheological properties at 25°C for the three solutions used in this work.

Results

Overall mass transfer coefficients for the transfer of carbon dioxide in pure water, 0.25, 0.50, and 0.55 wt. % aqueous Carbopol solutions are computed from the measurements of concentrations and flow rates of the fluid in the dialysis membrane section and annulus section, respectively. Turbulent mass transfer data for each of the solutions are taken by maintaining the flow rate in the annulus section constant while varying the flow rate in the dialysis membrane section. The mass flux is computed from experimental quantities by $N_A = F_1(C_2 - C_1)/A_{MT}$. The overall mass transfer coefficients are in turn computed from the definition $K_o = N_A/\Delta C_{lm}$.

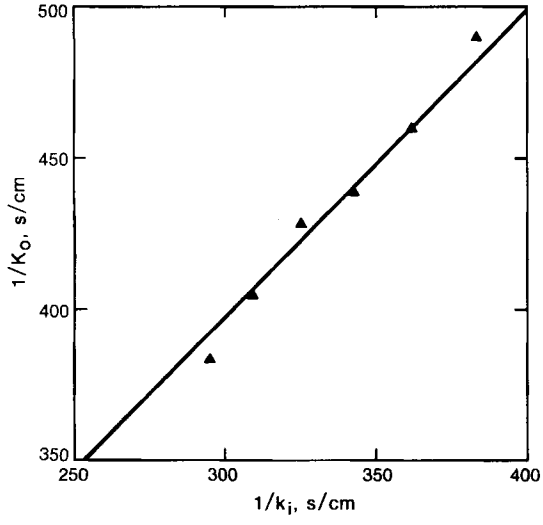

Figure 3. Modified Wilson plot for 0.5% carbopol solution.

The dialysis membrane section mass transfer coefficient, k_i, is obtained from the overall coefficient by a modified Wilson plot technique as follows. Because of the linearity between the mass transfer rate and the concentration profile, the overall resistance to mass transfer is a sum of the individual resistances to mass transfer in the membrane and annulus sections and resistance of the membrane.

$$\frac{1}{K_o} = \frac{1}{k_i} + \frac{1}{k_o} + \frac{1}{k_d} \tag{5}$$

The temperature and flow conditions in the annulus were kept constant in order to maintain constant physical properties. Under these circumstances, k_o and k_d remain constant (at unknown values) while k_i is a function of velocity only. Note that the generalized Schmidt number depends on velocity for a non-Newtonian material. By selecting a prediction equation for the inside mass transfer coefficient k_i, we can express the experimental $1/K_o$ values in terms of any model unknown coefficients and the unknown constant $(1/k_o + 1/k_d)$ and determine these quanti-

Table 2. Experimental Sherwood Numbers

n	Re	Sc	$f \times 10^3$	Sh
1.0	6,663	486	8.627	262.5
1.0	7,237	486	8.432	295.8
1.0	7,811	486	8.258	302.3
1.0	8,671	486	8.027	343.3
1.0	9,531	486	7.826	417.5
1.0	10,680	486	7.594	533.4
1.0	11,540	486	7.442	485.6
1.0	12,400	486	7.304	518.2
0.902	3,290	1,002	9.996	189.6
0.902	3,487	992	9.817	195.5
0.902	3,685	983	9.652	197.4
0.902	4,017	969	9.402	233.0
0.902	4,217	962	9.264	242.8
0.902	4,620	947	9.014	263.0
0.902	5,026	934	8.792	288.1
0.879	2,823	1,476	10.34	187.6
0.879	3,019	1,456	10.12	201.9
0.879	3,217	1,438	9.921	213.1
0.879	3,416	1,420	9.736	218.4
0.879	3,617	1,404	9.565	234.1
0.879	3,818	1,389	9.407	250.7
0.854	1,796	2,656	11.82	160.9
0.854	1,910	2,617	11.58	170.1
0.854	2,025	2,581	11.35	171.3
0.854	2,141	2,547	11.14	178.0
0.854	2,258	2,514	10.95	189.5
0.854	2,375	2,484	10.76	187.7

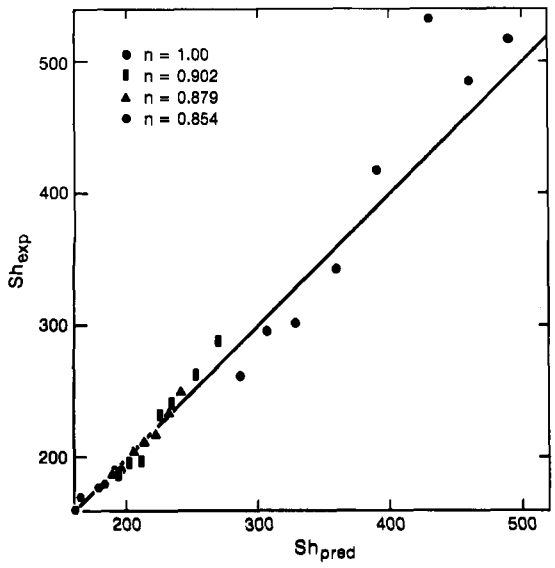

Figure 4. Comparison between predicted and experimental Sherwood numbers.

ties by least squares. Experimental values for k_i then follow by subtraction of $(1/k_o + 1/k_d)$ from $1/K_o$. In this work we predict k_i from Eq. 3, so that no "fitted" parameters are determined by the data. Figure 3 shows a modified Wilson plot for the mass transfer data obtained for the 0.5% Carbopol solution.

The experimental Sherwood numbers determined by this procedure are shown in Table 2. Figure 4 compares the experimental Sherwood numbers with those predicted by Eq. 3. It can be seen that the agreement between the observed Sherwood numbers and those predicted by Eq. 3 is generally very good; the mean absolute deviation between the 27 experimental and predicted points is 4.1%.

Notation

A_{MT} = mass transfer area, L^2
C_1 = membrane section inlet concentration, M/L^3
C_2 = membrane section outlet concentration, M/L^3
ΔC_{lm} = log mean concentration difference, M/L^3
d = tube diameter, L
D = diffusion coefficient, L^2/T
F_1 = membrane section flow rate, L^3/T
f = friction factor, Eq. 4
K = flow consistency index, M/LT^{2-n}
K_o = overall mass transfer coefficient, $N_A/\Delta C_{lm}$
k_d = mass transfer coefficient for membrane, L/T
k_i = mass transfer coefficient, membrane section, L/T
k_o = mass transfer coefficient, annulus section, L/T
n = non-Newtonian flow index
Pr = Prandtl number, ν^*/α
Re = Reynolds number, $D^n v_b^{2-n}\rho/[K(3n+1)/(4n)^n 8^{n-1}]$
Sc = Schmidt number, ν^*/D
Sh = Sherwood number, $k_i d/D$
St = Stanton number, k_i/v_b
v_b = bulk velocity, L/T
u^* = friction velocity, $\sqrt{f/2}\cdot v_b$, L/T
ρ = density, M/L^3
ν^* = effective kinematic viscosity, $(K/\rho)^{1/n}/u^{*(2-2n)/n}$

Literatured Cited

Dodge, D. W., and Metzner, A. B., "Turbulent Flow of Non-Newtonian Systems," *AIChE J.*, **5,** 189 (1959).

Hanna, O. T., and O. C. Sandall, "Developed Turbulent Transport in Ducts for Large Prandtl or Schmidt Numbers," *AIChE J.*, **18,** 527 (1972).

———, "Heat Transfer in Turbulent Pipe Flow for Liquids Having a Temperature-Dependent Viscosity," *ASME J. Heat Trans.*, **100,** 224 (1978).

———, "Turbulent Heat Transfer in a Circular Tube with Viscous Dissipation," *Chem. Eng. Comm.*, **18,** 163 (1982).

Hanna, O. T., O. C. Sandall, and P. R. Mazet, "Heat and Mass Transfer in Turbulent Flow Under Conditions of Drag Reduction," *AIChE J.*, **27,** 693 (1981).

Kafes, N. C., and C. W. Clump, "Turbulent and Laminar Mass Transfer in a Tubular Membrane," *AIChE J.*, **19,** 1247 (1973).

Kawase, Y., and J. J. Ulbrecht, "Mass and Heat Transfer in a Turbulent Non-Newtonian Boundary Layer," *Lett. Heat Mass Transf.*, **9,** 79 (1982).

Sandall, O. C., and O. T. Hanna, "Large Schmidt Number Mass Transfer in Turbulent Pipe Flow," *AIChE J.*, **25,** 190 (1979).

Sandall, O. C., O. T. Hanna, and M. Gelibter, "Non-Netwonian Turbulent Transport in a Circular Tube," *AIChE J.*, **22,** 1142 (1976).

Sandall, O. C., O. T. Hanna, and P. R. Mazet, "A New Theoretical Formula for Turbulent Heat and Mass Transfer with Gases or Liquids in Tube Flow," *Canad. J. Chem. Eng.*, **58,** 443 (1980).

Sandall, O. C., O. T. Hanna, and F. J. Valeri, "Heat Effects for Physical and Chemical Absorption in Turbulent Liquid Films," *Chem. Eng. Comm.*, **16,** 135 (1982).

Sandall, O. C., O. T. Hanna, and C. L. Wilson, "Heat Transfer across Turbulent Falling Liquid Films," *AIChE Symp. Ser.* No. 236, **80,** 3 (1984).

Manuscript received Aug. 22, 1985, and revision received Nov. 20, 1985.